AD_____
                                    (Leave blank)

Award Number:

W81XWH-06-1-0042

TITLE:

Molecular Imaging of Ovarian Carcinoma Angiogenesis

PRINCIPAL INVESTIGATOR:

Xiaoyuan Chen, PhD

CONTRACTING ORGANIZATION:
Stanford University,
Menlo Park, California 94025-3434

REPORT DATE:

March 2009

TYPE OF REPORT:

Revised Final report

PREPARED FOR: U.S. Army Medical Research and Materiel Command
               Fort Detrick, Maryland 21702-5012

DISTRIBUTION STATEMENT: (Check one)

     X Approved for public release; distribution unlimited

     ☐ Distribution limited to U.S. Government agencies only;
        report contains proprietary information

The views, opinions and/or findings contained in this report are
those of the author(s) and should not be construed as an official
Department of the Army position, policy or decision unless so
designated by other documentation.

REPORT DOCUMENTATION PAGE		*Form Approved* *OMB No. 074-0188*

Public reporting burden for this collection of information is estimated to average 1 hour per response, including the time for reviewing instructions, searching existing data sources, gathering and maintaining the data needed, and completing and reviewing this collection of information. Send comments regarding this burden estimate or any other aspect of this collection of information, including suggestions for reducing this burden to Washington Headquarters Services, Directorate for Information Operations and Reports, 1215 Jefferson Davis Highway, Suite 1204, Arlington, VA 22202-4302, and to the Office of Management and Budget, Paperwork Reduction Project (0704-0188), Washington, DC 20503

1. Agency Use Only (Leave blank)	2. Report Date March 2009	3. Report Type and Period Covered (1 February 2006- 31 January 2009) Final report	
4. Title and Subtitle Molecular Imaging of Ovarian Carcinoma Angiogenesis		**5. Award Number** **W81XWH-06-1-0042**	
6. Author(s) Xiaoyuan Chen, PhD			
7. Performing Organization Name (Include Name, City, State, Zip Code and Email for Principal Investigator) Stanford University, Stanford, CA 94305 E**-Mail: shawn.chen@nih.gov**		**8. Performing Organization Report Number (Leave Blank)**	
9. Sponsoring/Monitoring Agency Name and Address U.S. Army Medical Research and Materiel Command Fort Detrick, Maryland 21702-5012		**10. Sponsoring/Monitoring Agency Report Number (Leave Blank)**	
11. Supplementary Notes (i.e., report contains color photos, report contains appendix in non-print form, etc.)			
12a. Distribution/Availability Statement (check one) x Approved for public release; distribution unlimited ☐ Distribution limited to U.S. Government agencies only - report contains proprietary information		**12b. Distribution Code** (Leave Blank)	

13. Abstract *(Maximum 200 Words)* *(abstract should contain no proprietary or confidential information)*

This purpose of this proposal is to use high resolution microPET technology to image ovarian cancer integrin $\alpha_v\beta_3$ expression in vivo. Ovarian cancer is angiogenesis dependent. Integrin $\alpha_v\beta_3$, a key player in tumor angiogenesis and metastasis, has been identified as a target for diagnostic and therapeutic interventions for several highly proliferative and metastatic tumor types. **Specific Aim 1:** To develop and optimize ^{18}F-labeled RGD peptides for ovarian carcinoma targeting. **Specific Aim 2:** To test ^{18}F-RGD peptide tracers in ovarian carcinoma models of different tumor integrin $\alpha_v\beta_3$ expression levels in order to correlate the magnitude of tumor uptake with receptor density. **Major Findings:** In year 1, we have synthesized a series of multimeric RGD peptides with high integrin $\alpha_v\beta_3$ affinity/specificity and labeled these peptides with F-18 for PET imaging of integrin expression in vivo (Aim 1). In year 2, we have also established several ovarian cancer models with differentiated integrin levels (Aim 2). One of the dimeric RGD peptide tracer 18F-FPRGD2 with high tumor targeting efficacy and favorable in vivo kinetics has been identified as the lead compound for future translational work.

14. Subject Terms (keywords previously assigned to proposal abstract or terms which apply to this award)			**15. Number of Pages (count all pages including appendices)**
			16. Price Code (Leave Blank)
17. Security Classification of Report Unclassified	**18. Security Classification of this Page** Unclassified	**19. Security Classification of Abstract** Unclassified	**20. Limitation of Abstract** Unlimited

NSN 7540-01-280-5500

Standard Form 298 (Rev. 2-89)
Prescribed by ANSI Std. Z39-18
**298-102**

Table of Contents

INTRODUCTION

Ovarian epithelial carcinomas are characterized by local proliferation and invasion of ovarian surface epithelium (OSE)-derived tumor cells, followed frequently by dissemination in the peritoneal cavity and formation of ascites containing clusters of tumor cells. This cancer is therefore characterized by the presence of two forms of call populations, some growing as solid tumors and others in suspension (*1*). At each step of malignant progression, adhesive mechanisms plays an important role, and integrins are likely to participate in these events (*2-8*). In most ovarian cancer cells, integrin $\alpha_v\beta_3$ is expressed and its ligand vitronectin is synthesized as a primary adhesion substrate. In fact, integrin $\alpha_v\beta_3$ is found at a significantly higher rate in primary ovarian cancer than in ovarian tumors of low malignant potential, a fact which points to a role of $\alpha_v\beta_3$ during ovarian cancer progression. Although the precise mechanism of tumor progression promoted via $\alpha_v\beta_3$ is still rather inconclusive, various studies support a potential role of $\alpha_v\beta_3$ in selective invasion and the generation of growth and survival signals (*9-12*). A recent study evidenced the correlation between α_v-integrin expression and poor survival in ovarian carcinoma (*11*). Given that the initial critical step of ovarian cancer metastasis is the attachment of cancer cells onto the peritoneum or omentum, in addition to the proven positive clinical results of anti-angiogenic therapy, targeting integrins is likely to be one of the most feasible approaches (*13*).

The ability to non-invasively visualize and quantify $\alpha_v\beta_3$ integrin expression level will provide new opportunities to document tumor (tumor cells and sprouting tumor vasculature) receptor expression, more appropriately select patients considered for anti-integrin treatment and monitor treatment efficacy in integrin-positive patients (*14-17*). In the past few years, we have developed a series of peptide and antibody based probes for multimodality imaging of integrin expression in vivo. This annual report will only summarize the progress highly relevant to this OCRP pilot proposal. We hypothesize that ovarian cancer integrin expression can be visualized and quantified with suitably labeled RGD peptide antagonist of integrin $\alpha_v\beta_3$ and that the magnitude of tumor uptake from non-invasive molecular imaging may be well-correlated with tumor integrin expression levels.

BODY

Chemistry and Radiochemistry

During year 1 of the funding period, we have reported the development of RGD monomer, dimer, and tetramer labeled with ^{18}F using N-succinimidyl-4-^{18}F-fluorobenzoate (^{18}F-SFB) as the synthon. However, this procedure suffers from lengthy and tedious multistep synthetic procedures. As a result, it is challenging to automate and adversely decrease the overall radiolabeling yield. Nevertheless, the lead compound ^{18}F-FB-mini-PEG-E[c(RGDyK)]₂ (^{18}F-FPRGD2) is currently being translated into clinic for first-in-human studies.
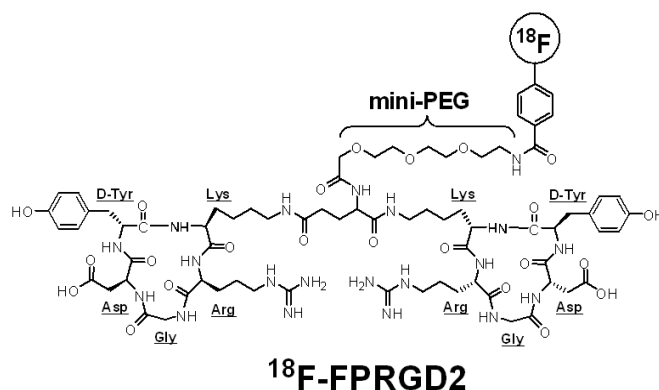
Fig. 1. Schematic structure of ^{18}F-FPRGD2.

The recent discovery that Cu(I) catalyzes the Huisgen 1,3-dipolar cycloaddition of organo azides with terminal alkynes to form 1,2,3-triazoles (*18, 19*), often referred to as 'click chemistry' (*20*), has led to wide applications in combinatorial chemistry (*21-23*). This reaction could be carried out in high yields under mild conditions, and the 1,2,3-triazole formed has similar polarity and size with amide bond (*24*). Due to these favorable aspects with 'click chemistry', the use of this reaction for making ^{18}F labeled RGD peptides have been successfully conducted in our lab.

As shown in Fig. 1, both alkyne-tosylate (**1**) and azido-RGD2 were obtained in high yields. The alkyne-fluoride was prepared in situ and could be used directly for the reaction with azido-RGD2 to make the cold standard, which was purified by HPLC and confirmed by MALDI-TOF mass spectrometry. The radiochemical purity of the ^{18}F-labeled peptide ^{18}F-FPTA-RGD2 was higher than 97% according to analytical HPLC. The specific radioactivity of ^{18}F-FPTA-RGD2 was determined to be about 100–200 TBq/mmol, as the unlabeled azido-RGD2 was efficiently separated from the product.

4
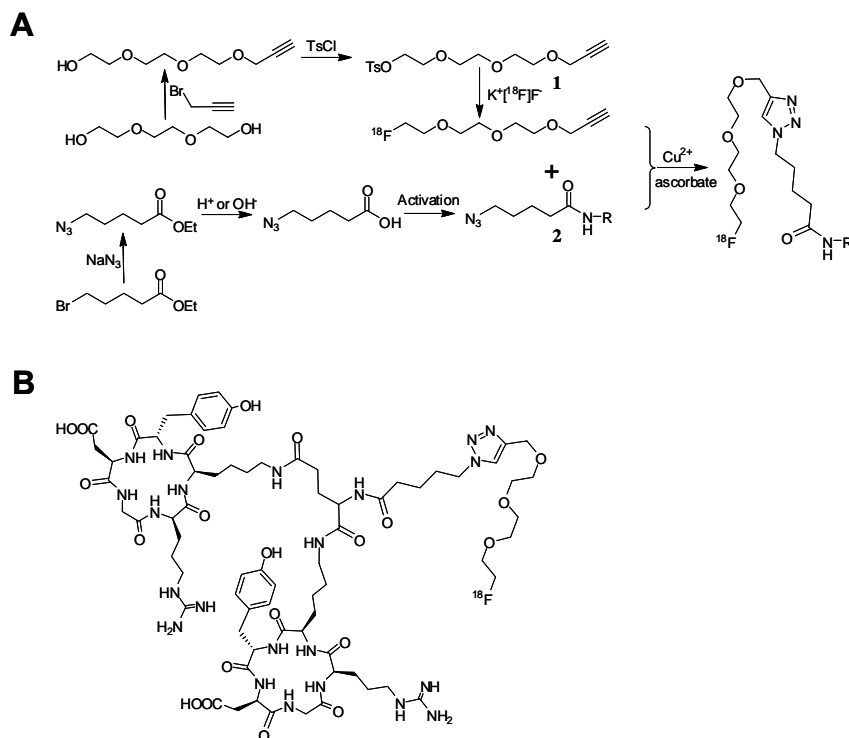
Figure 1. (A) Radiosynthesis of ^{18}F-fluoro-PEG-alkyne intermediate and 1.3-dipolar cycloaddition with terminal azide. R = targeting biomolecule (peptides, proteins, antibodies et al.). (B) Structure of ^{18}F-fluoro-PEG-alkyne labeled E[c(RGDyK)]$_2$: ^{18}F-fluoro-PEG-triazole-E(RGDyK)$_2$ (^{18}F-FPTA-RGD2).

The octanol/water partition coefficient (logP) for ^{18}F-FPTA-RGD2 was -2.71$\pm$0.006, indicating that the tracer is slightly more hydrophilic than [18]F-FB-RGD2 ([18]F-FRGD2, -2.103$\pm$0.030) and [18]F-FB-PEG3-RGD2 ([18]F-FPRGD2, -2.280$\pm$0.054) (*25*).

In vitro Cell Integrin Receptor-Binding Assay

The receptor-binding affinity of RGD2 and FPTA-RGD2 was determined by performing competitive displacement studies with ^{125}I-echistatin. All peptides inhibited the binding of ^{125}I-echistatin (integrin $\alpha_v\beta_3$ specific) to U87MG cells in a concentration dependent manner. The IC$_{50}$ values for RGD2 and FPTA-RGD2 were 79.2 ± 4.2 and 144 ± 6.5 nM, respectively (n = 3) (Fig. 2). In a parallel experiment, the IC$_{50}$ value for FPRGD2 was 97 ± 4.8 nM. The comparable IC$_{50}$ values of these compounds suggest that the introduction of miniPEG linker and triazole group had little effect on the receptor binding affinity.
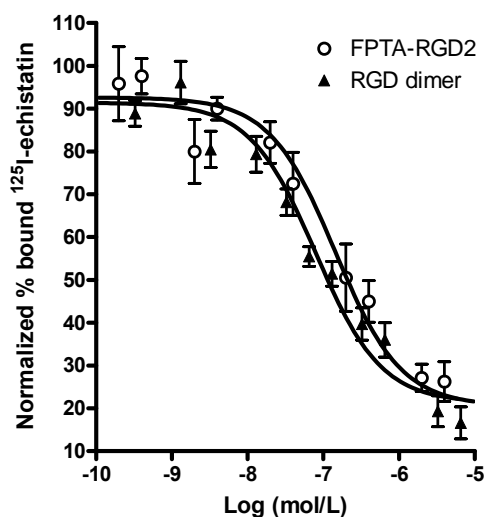

Figure 2. Cell binding assay of E[c(RGDyK)]$_2$ and FPTA-RGD2 using U87MG cells with competitive displacement studies using ^{125}I-echistatin. The IC$_{50}$ values for E[c(RGDyK)]$_2$ and FPTA-RGD2 were 79.2 ± 4.2 and 144 ± 6.5 nM, respectively (n = 3).

microPET Imaging Studies

Dynamic microPET scans were performed on U87MG xenograft model and selected coronal images at different time points after injecting ^{18}F-FPTA-RGD2 were shown in Figure 3A. Good tumor-to-contralateral background contrast was observed as early as 10 min after injection (5.4 ± 0.7 %ID/g). The U87MG tumor uptake was 3.1 ± 0.6, 2.1 ± 0.4, and 1.3 ± 0.4 %ID/g at 0.5, 1, and 2 h p.i., respectively (n = 3). Most activity in the non-targeted tissues and organs were cleared by 1 h p.i. For example, the uptake values in the kidney, liver, and muscle were as low as 2.7 ± 0.8, 1.9 ± 0.4, and 1.0 ± 0.3 %ID/g, respectively at 1 h p.i. ^{18}F-FPTA-RGD2 was cleared mainly through the kidneys. Some hepatic clearance was also observed. The integrin $\alpha_v\beta_3$ specificity of ^{18}F-FPTA-RGD2 in vivo was confirmed by a blocking experiment where the tracer was co-injected with c(RGDyK) (10 mg/kg). As can be seen from Figure 3B, the U87MG tumor uptake in the presence of non-radiolabeled RGD peptide (0.9 ± 0.3 %ID/g) is significantly lower than that without RGD blocking (2.1 ± 0.4 %ID/g) (P < 0.05) at 1 h p.i.

6
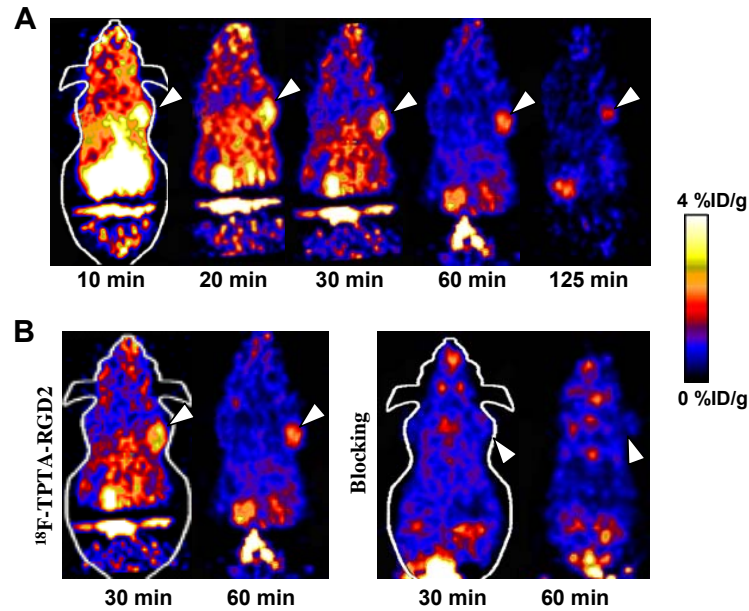
Figure 3. (A) Decay-corrected whole-body coronal microPET images of athymic female nude mice bearing U87MG tumor at 10, 20, 30, 60 and 125 min post-injection (p.i.) of about 2 MBq of ^{18}F-FPTA-RGD2. (B) Coronal microPET images of U87MG tumor-bearing mice at 30 and 60 min p.i. of ^{18}F-FPTA-RGD2 with (denoted as "Blocking") and without coinjection of 10 mg/kg mouse body weight of c(RGDyK). Tumors are indicated by arrows.
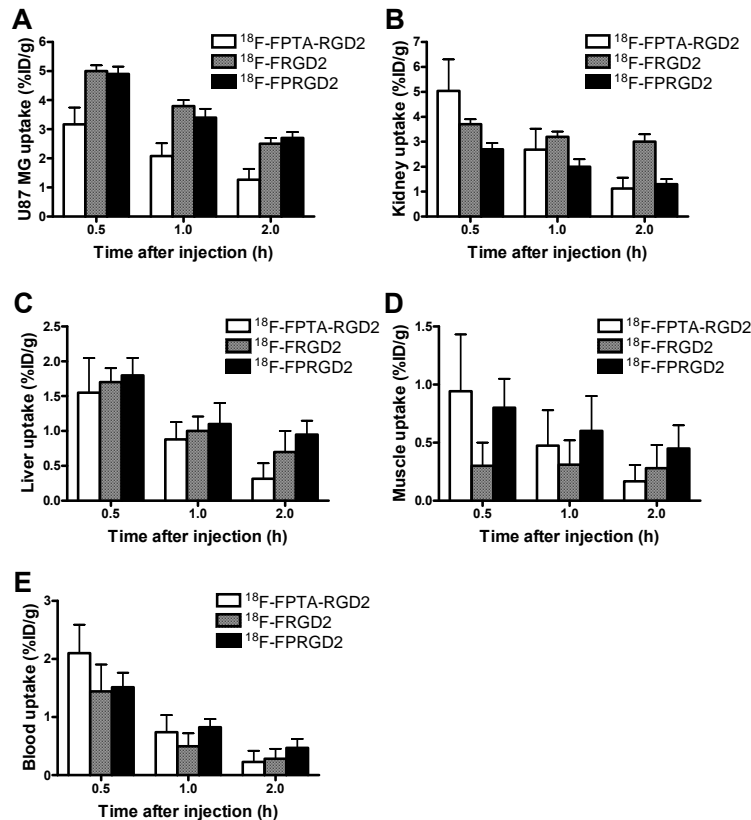
Figure 4. Comparison of ^{18}F-FPTA-RGD2, ^{18}F-FB-RGD2 (^{18}F-FRGD2) and ^{18}F-FB-PEG3-RGD2 (^{18}F-FPRGD2) in U87MG tumor, kidney, liver, muscle, and blood over time.

The comparison of tumor and various organ uptake of ^{18}F-FPTA-RGD2 with ^{18}F-FPRGD2 and ^{18}F-FRGD2 were shown in Figure 5. The uptake in the U87MG tumor was slightly lower for ^{18}F-FPTA-RGD2 which might be caused by integrin $\alpha_v\beta_3$ binding affinity difference (Fig. 4A). The kidney uptake for these three tracers was comparable (Fig. 4B) and the clearance rate was highest for ^{18}F-FPTA-RGD2. ^{18}F-FPTA-RGD2 had lowest liver uptake which was consistent with the hydrophilic sequence of these three compounds (Fig. 4C). The non-specific uptake in the muscle was at a very low level for all three compounds (Fig. 4D).

In Vivo Metabolic Stability Studies

The metabolic stability of ^{18}F-FPTA-RGD2 was determined in mouse blood and urine and the in liver, kidney and tumor homogenates at 1 h after intravenous injection of radiotracer into a U87MG tumor-bearing mouse. The extraction efficiency of all organs was between 86% and 99% (Table 2). The lowest extraction efficiency was found for the kidney. There are 1% to 41% of the total activity could not be trapped on the C-18 cartridges, which can be related to very hydrophilic metabolites and protein-bound activity. After ACN elution, the radioactivity of each sample was injected onto an analytical HPLC and the HPLC chromatograms are shown in Figure 6. The fraction of intact tracer was between 75 % and 99 % (Table 2). Although we did not identify the metabolites, we found that all metabolites eluted earlier from the HPLC column than the parent compound (Fig. 5), which behaved similarly to ^{18}F-FRGD2 (*26*) and ^{18}F-FPRGD2 (*25*).

Table 2. Extraction efficiency, elution efficiency, and HPLC analysis of soluble fraction of tissue homogenates at 1 h post-injection of ^{18}F-FPTA-RGD2.

Fraction	Blood	Urine	Liver	Kidney	U87MG
Extraction efficiency (%)					
Insoluble fraction	0.8	ND	10.3	13.3	7.5
Soluble fraction	99.2	ND	89.7	86.7	92.5
Elution efficiency (%)					
Unretained fraction	2.8	0.4	33.9	12.8	18.5
Wash water	8.8	0.5	7.4	3.9	5.2
Acetonitrile eluent	88.4	99.1	58.7	83.3	76.4
HPLC analysis (%)					
Intact tracer	75.9	99.7	81.6	89.1	82.4
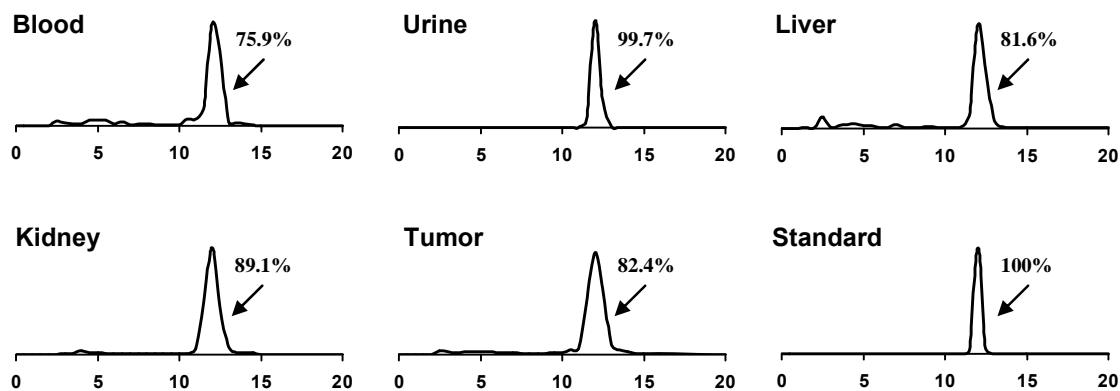
Figure 5. Metabolic stability of ^{18}F-FPTA-RGD2 in mouse blood and urine samples and in liver, kidney and U87MG tumor homogenates at 1 h after injection. The HPLC profile of pure ^{18}F-FPTA-RGD2 (Standard) is also shown.

KEY ACCOMPLISHMENTS

- A lead compound ^{18}F-FB-mini-PEG-E[c(RGDyK)]$_2$ (^{18}F-FPRGD2) was identified from a library of RGD peptides for positron emission tomography (PET) imaging of tumor integrin expression.
- A novel click chemistry strategy was applied to label RGD peptides with ^{18}F with shorter reaction time and easier chemistry than traditional ^{18}F-SFB synthon.
- Suitably labeled RGD peptides are metabolically stable with favorable pharmacokinetics and ability to reflect integrin receptor status in vivo.

REPORTABLE OUTCOMES

Publications:

Wu Z, Li Z-B, Cai W, Chin FT, Li F, <u>Chen X</u>
^{18}F-labeled mini-PEG spacered RGD dimer (^{18}F-FPRGD2): synthesis and microPET imaging of $\alpha_v\beta_3$ integrin expression
Eur J Nucl Med Mol Imaging 2007;34(11):1823-1831.

Wu Z, Li Z-B, Cai W, He L, Chin FT, Li F, <u>Chen X</u>
microPET Imaging of Tumor $\alpha_v\beta_3$ Integrin Expression Using ^{18}F-labeled PEGylated Tetrameric RGD Peptide (^{18}F-FPRGD4)
J Nucl Med, 2007;48:1536-44.

Li ZB, Wu Z, Chen K, Chin FT, <u>Chen X</u>.
Click Chemistry for ^{18}F-Labeling of RGD Peptides and microPET Imaging of Tumor Integrin alphavbeta3 Expression
Bioconjug Chem 2007;18(6):1987-1994.

Liu S, Liu Z, Chen K, Yan Y, Watzlowik P, Wester HJ, Chin FT, <u>Chen X</u>.
^{18}F-labeled galacto and PEGylated RGD dimers for PET imaging of $\alpha v\beta 3$ integrin expression.
Mol Imaging Biol. 2010;12(5):530-8.

Liu Z, Liu S, Wang F, Liu S, <u>Chen X</u>
Noninvasive imaging of tumor integrin expression using (18)F-labeled RGD dimer peptide with PEG (4) linkers.
Eur J Nucl Med Mol Imaging. 2009;36(8):1296-307

Conference Abstracts:

Li Z-B, Wu Z, Chen K, Chin FT, <u>Chen X</u>
Click Chemistry for ^{18}F-Labeling of RGD Peptides and microPET Imaging of Tumor $\alpha v\beta 3$ Integrin Expression
Joint Molecular Imaging Conference, Providence, Rhode Island, September 2007

CONCLUSIONS

In conclusion, we identified a lead compound ^{18}F-FB-mini-PEG-E[c(RGDyK)]$_2$ (^{18}F-FPRGD2) from a library of RGD peptides for positron emission tomography (PET) imaging of tumor integrin expression. We also developed a novel click chemistry strategy to label dimeric RGD peptide for tumor integrin expression imaging. Suitably labeled RGD peptides appear to be metabolically stable with favorable pharmacokinetics and ability to reflect integrin receptor status in vivo.

REFERENCES

1. Hamilton TC. Ovarian cancer, Part I: Biology. *Curr Probl Cancer.* Jan-Feb 1992;16(1):1-57.

2. Moser TL, Pizzo SV, Bafetti LM, Fishman DA, Stack MS. Evidence for preferential adhesion of ovarian epithelial carcinoma cells to type I collagen mediated by the alpha2beta1 integrin. *Int J Cancer.* Sep 4 1996;67(5):695-701.

3. Cruet S, Salamanca C, Mitchell GW, Auersperg N. alphavbeta3 and vitronectin expression by normal ovarian surface epithelial cells: role in cell adhesion and cell proliferation. *Gynecol Oncol.* Nov 1999;75(2):254-260.

4. Carreiras F, Denoux Y, Staedel C, Lehmann M, Sichel F, Gauduchon P. Expression and localization of alpha v integrins and their ligand vitronectin in normal ovarian epithelium and in ovarian carcinoma. *Gynecol Oncol.* Aug 1996;62(2):260-267.

5. Cannistra SA, Ottensmeier C, Niloff J, Orta B, DiCarlo J. Expression and function of beta 1 and alpha v beta 3 integrins in ovarian cancer. *Gynecol Oncol.* Aug 1995;58(2):216-225.

6. Bartolazzi A, Cerboni C, Flamini G, Bigotti A, Lauriola L, Natali PG. Expression of alpha 3 beta 1 integrin receptor and its ligands in human lung tumors. *Int J Cancer.* Aug 22 1995;64(4):248-252.

7. Liapis H, Adler LM, Wick MR, Rader JS. Expression of alpha(v)beta3 integrin is less frequent in ovarian epithelial tumors of low malignant potential in contrast to ovarian carcinomas. *Hum Pathol.* Apr 1997;28(4):443-449.

8. Goldberg I, Davidson B, Reich R, et al. Alphav integrin expression is a novel marker of poor prognosis in advanced-stage ovarian carcinoma. *Clin Cancer Res.* Dec 2001;7(12):4073-4079.

9. van der Flier A, Sonnenberg A. Function and interactions of integrins. *Cell Tissue Res.* Sep 2001;305(3):285-298.

10. Hapke S, Kessler H, Luber B, et al. Ovarian cancer cell proliferation and motility is induced by engagement of integrin alpha(v)beta3/Vitronectin interaction. *Biol Chem.* Jul 2003;384(7):1073-1083.

11. Davidson B, Goldberg I, Reich R, et al. AlphaV- and beta1-integrin subunits are commonly expressed in malignant effusions from ovarian carcinoma patients. *Gynecol Oncol.* Aug 2003;90(2):248-257.

12. Cruet-Hennequart S, Maubant S, Luis J, Gauduchon P, Staedel C, Dedhar S. alpha(v) integrins regulate cell proliferation through integrin-linked kinase (ILK) in ovarian cancer cells. *Oncogene.* Mar 20 2003;22(11):1688-1702.

13. Sawada K, Ohyagi-Hara C, Kimura T, Morishige K. Integrin inhibitors as a therapeutic agent for ovarian cancer. *J Oncol.* 2012;2012:915140.

14. Chen X. Multimodality imaging of tumor integrin alphavbeta3 expression. *Mini Rev Med Chem.* Feb 2006;6(2):227-234.

15. Cai W, Gambhir SS, Chen X. Multimodality tumor imaging targeting integrin $\alpha_v\beta_3$. *Biotechniques.* 2005;39:S6-S17.

16. Morrison M, Cuthbertson A. Integrin imaging to evaluate treatment response. *Theranostics.* 2011;1:149-153.

17. Zhang Y, Yang Y, Cai W. Multimodality Imaging of Integrin alpha(v)beta(3) Expression. *Theranostics.* 2011;1:135-148.

18. Tornoe CW, Christensen C, Meldal M. Peptidotriazoles on solid phase: [1,2,3]-triazoles by regiospecific copper(i)-catalyzed 1,3-dipolar cycloadditions of terminal alkynes to azides. *J Org Chem.* May 3 2002;67(9):3057-3064.

19. Rostovtsev VV, Green LG, Fokin VV, Sharpless KB. A stepwise huisgen cycloaddition process: copper(I)-catalyzed regioselective "ligation" of azides and terminal alkynes. *Angew Chem Int Ed Engl.* Jul 15 2002;41(14):2596-2599.

20. Kolb HC, Finn MG, Sharpless KB. Click Chemistry: Diverse Chemical Function from a Few Good Reactions. *Angew Chem Int Ed Engl.* Jun 1 2001;40(11):2004-2021.

21. Pagliai F, Pirali T, Del Grosso E, et al. Rapid synthesis of triazole-modified resveratrol analogues via click chemistry. *J Med Chem.* Jan 26 2006;49(2):467-470.

22. Burley GA, Gierlich J, Mofid MR, et al. Directed DNA metallization. *J Am Chem Soc.* Feb 8 2006;128(5):1398-1399.

23. Krasinski A, Radic Z, Manetsch R, et al. In situ selection of lead compounds by click chemistry: target-guided optimization of acetylcholinesterase inhibitors. *J Am Chem Soc.* May 11 2005;127(18):6686-6692.

24. Bock VD, Hiemstra H, van Maarseveen JH. Cu^I-Catalyzed alkyne-azide "Click" cycloadditions form a mechanistic and synthetic perspective. *Eur J Org Chem.* 2006:51-68.

25. Wu Z, Li Z, Cai W, et al. 18F-labeled mini-PEG spacered RGD dimer (18F-FPRGD2): synthesis and microPET imaging of αvβ3 integrin expression. *Eur J Nucl Med Mol Imaging.* 2007;IN PRESS.

26. Zhang X, Xiong Z, Wu Y, et al. Quantitative PET imaging of tumor integrin alphavbeta3 expression with 18F-FRGD2. *J Nucl Med.* Jan 2006;47(1):113-121.

APPENDICES

N/A